Langmuir

ARTICLE

pubs.acs.org/Langmuir

Engineered Alginate Hydrogels for Effective Microfluidic Capture and Release of Endothelial Progenitor Cells from Whole Blood

Adam Hatch,[†] Georg Hansmann,[‡] and Shashi K. Murthy*[,†]

[†]Department of Chemical Engineering, Northeastern University, Boston, Massachusetts 02115, United States

[‡]Department of Cardiology, Children's Hospital Boston and Harvard Medical School, Boston, Massachusetts 02115, United States

Supporting Information

ABSTRACT: Microfluidic adhesion-based cell separation systems are of interest in clinical and biological applications where small sample volumes must be processed efficiently and rapidly. While the ability to capture rare cells from complex suspensions such as blood using microfluidic systems has been demonstrated, few methods exist for rapid and nondestructive release of the bound cells. Such detachment is critical for applications in tissue engineering and cell-based therapeutics in contrast with diagnostics wherein immunohistochemical, proteomic, and genomic analyses can be carried out by simply lysing captured cells. This paper demonstrates how the incorporation of four-arm amine-terminated poly(ethylene glycol) (PEG) molecules along with antibodies within alginate hydrogels can enhance the ability of the hydrogels to capture endothelial progenitor cells (EPCs) from whole human blood. The hydrogel coatings are applied conformally onto pillar structures within microfluidic channels and their dissolution with a chelator allows for effective recovery of EPCs following capture.

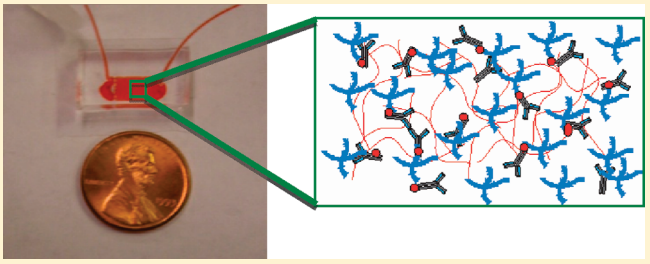

INTRODUCTION

The use of microfluidic devices in adhesion-based separation of cells is an active area of research in both clinical medicine and basic science.[1−4] This mode of separation is attractive because no labeling with fluorescent or magnetic tags is needed to drive the separation process, unlike conventional fluorescence- or magnet-activated cell sorting (FACS and MACS, respectively). The high surface area to volume ratios of microfluidic channels together with the ability to enhance surface area with microfabricated structures[3,5,6] has enabled such devices to capture cells of extremely low concentrations for a broad range of applications. A major challenge in this area, however, is the lack of methods to achieve nondestructive release of cells captured within microfluidic channels.[7−10] In a diagnostic context, useful information can be obtained by simple adhered cell counts[2,3] or by lysing cells on a chip and performing proteomic and/or genomic analysis.[3,4] However, when isolated cells need to be recovered for therapeutic or scientific purposes, cell detachment must be carried out without causing physical damage and changes in phenotypic identity or function in the cells. These constraints limit the chemical and mechanical forces that can be applied to achieve cell release; for example, enzyme-induced cell detachment is known to cause chemical and phenotypic changes within cells.[9,10] Furthermore, when simplicity is desired for devices designed for point-of-care and disposable use, the use of electrical, thermal, or optical means of cell detachment becomes infeasible.[11,12]

In previous work, we have described how alginate hydrogel coatings can be formed on the inner surfaces of microfluidic channels[12] and utilized for cell capture from flowing suspensions followed by release. These coatings contained cell-adhesive molecules covalently bound to the carboxylic acid groups of alginic acid. While these coatings were able to achieve capture and release of primary rat cardiac fibroblasts from homogeneous suspensions, the adhesion of the cells to alginate hydrogels containing no cell-adhesive molecules was fairly high. High baseline adhesion levels are undesirable when cell capture must be carried out from heterogeneous suspensions of cells, particularly when target cell concentrations are low. As a material, however, alginate hydrogels are easy to create via physical cross-linking in the presence of divalent cations and dissolve using relatively low concentrations of chelator molecules, such as ethylenediaminetetraacetic acid (EDTA). In the context of microfluidic devices and as shown in our prior work,[12] these hydrogels can be created by adsorbing functionalized alginic acid within the microchannels and then forming the gel by flowing a solution of calcium chloride. The concentration of alginic acid in the initial step must be low enough to enable injection into a narrow channel and the flow rate of calcium chloride in the next step must be high enough to ensure that the gel does not fill the entire channel. These parameters can be easily optimized, and the noncovalent nature of the hydrogel−microchannel binding

Received: December 18, 2010
Revised: February 8, 2011
Published: March 14, 2011

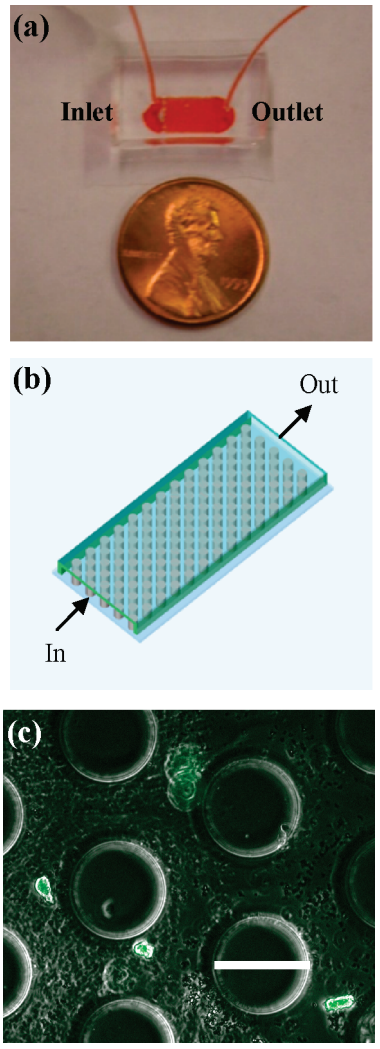

Figure 1. Image of cell capture device (a) and schematic diagram of the microfluidic post array (b). EPCs captured within the device (c), where green represents staining with fluorescently labeled anti-CD133 (scale bar =100 μm).

allows extension of the coating process to microchannels made of any material.

This paper examines how alginate hydrogels can be modified with four-arm poly(ethylene glycol) (PEG) molecules to enhance functionalization with cell-adhesive antibodies while simultaneously suppressing nonspecific binding. The effectiveness of these functionalized hydrogels as capture/release coatings is demonstrated by targeting endothelial progenitor cells (EPCs) from whole human blood using a pillar-array microfluidic device. EPCs are present at relatively low concentrations in blood, with typical concentrations in the range of 10 000 cells/mL in healthy individuals (as measured in our laboratory). The isolation of these cells from blood is a first step in the growth of blood vessels in vitro[13] and is typically carried out using a multiple-cycle technique of centrifugation and plating. Our work is motivated by the need for more rapid and low-cost methods of isolation of EPCs and other rare cells utilized in tissue engineering and cell-based regenerative repair.

The incorporation of PEG within alginate hydrogels for three-dimensional cell culture or drug delivery is well-established;[14,15] however, the use of these hydrogels in cell-affinity chromatography is relatively new. This paper demonstrates how four-arm, amine-terminated PEG molecules can not only increase the purity of captured EPCs by suppression of nonspecific binding but also enhance capture yield by providing more tether points for capture antibodies.

MATERIALS AND METHODS

Materials. Glass slides, EDC [1-ethyl-3-(3-dimethylaminopropyl)carbodiimide hydrochloride], sulfo-NHS (*N*-hydroxysuccinimide), EDTA, 2-(4-morpholino)ethanesulfonic acid (MES) buffer, a micro bicinchoninic acid (BCA) protein assay kit, and heparin vacuum tubes were purchased from Fisher Scientific (Fair Lawn, NJ). For microfluidic device fabrication, SU-8 photoresist and developer were obtained from MicroChem (Newton, MA); silicone elastomer and curing agent were obtained from Dow Corning (Midland, MI). Phosphate-buffered saline (PBS; 1×, without calcium or magnesium) was purchased from Mediatech (Herndon, VA). The capture antibody, monoclonal mouse antihuman CD34, and goat antihuman Flk-1 were obtained from Santa Cruz Biotechnology (Santa Cruz, CA). Mouse antihuman CD133-PE, mouse antihuman CD45-FITC, and mouse antigoat IgG-PerCP antibodies were obtained from eBioscience (San Diego, CA). Rabbit IgG was purchased from Vector Laboratories (Burlingame, CA). Calcium chloride dehydrate, Trypan Blue solution, and alginic acid were purchased from Sigma (St. Louis, MO). Amine-terminated four-arm PEG ($PEG\text{-}NH_2$) with molecular weights of 10 000 (10K MW) and 20 000 (20K MW) was purchased from Laysan Bio (Arab, AL).

Microfluidic Cell Capture Device Design. The device uses a post array design similar to that used by Nagrath et al.[3] (Figure 1a,b). To achieve disruption of flow streams and achieve optimal capture, the posts were arranged in a hexagonal layout, as described by Gleghorn et al.[6] The posts have a diameter of 100 μm and a transverse spacing of 150 μm from center to center (Figure 1c). Rows have a center-to-center spacing of 125 μm and each is offset by 50 μm. The post array is 0.7 cm long and 0.5 cm wide. The posts height was approximately 50 μm for the devices fabricated by soft lithography as described below.

Microfluidic Device Fabrication. A two-dimensional projection of the cell capture device was drawn using AutoCAD in-house, and the image was imprinted at high resolution onto a chrome mask by FineLine Imaging (Colorado Springs, CO). This photomask was utilized to generate a negative master at the George J. Kostas Nanoscale Technology and Manufacturing Research Center at Northeastern University. In précis, a silicon wafer was coated with SU 8-50 photoresist to a thickness of approximately 50 μm. With the mark overlaid, the wafer was exposed to 365 nm, 11 mW/cm^2 ultraviolet light from a Q2001 mask aligner (Quintel Co., San Jose, CA). Unexposed photoresist was then removed using SU 8 developer.

For poly(dimethylsiloxane) (PDMS) device fabrication, the silicone elastomer and curing agent were mixed in a 10:1 (w/w) ratio and poured on top of the negative master wafers, degassed, and allowed to cure overnight at 65 °C. PDMS replicas were then pulled off the wafers prior to punching inlet and outlet holes with a 19-gauge blunt-nose needle. The replicas and glass slides were exposed to oxygen plasma (50 mW with 8% oxygen for 30 s) in a PX-250 plasma chamber (March Instruments, Concord, MA) and then immediately placed in contact with each other. The irreversible bonding between PDMS and glass was completed by baking for 5 min at 65 °C.

PEG/Antibody-Functionalized Hydrogel Synthesis. Seven different hydrogel formulations were investigated in this study and these are designated as gel types I−VII. For gel type I, 45 mg of alginic acid, 4.8 mg of EDC, 13.2 mg of sulfo-NHS, and 20 μL of inert IgG (1 g/mL) were added to 2 mL of MES buffer solution and mixed using an IKA Ultra Turrax tube disperser (Wilmington, NC) for 29 min and allowed to incubate for 60 min. For gel type II, 45 mg of alginic acid, 4.8 mg of EDC, 13.2 mg of sulfo-NHS, and 100 μL of antihuman CD34 (200 μg/

Table 1. Summary of Synthesis Protocols for Different Hydrogel Formulations

		components in each mixing sequence[a]				mixing/incubation times (min)	
gel type	PEG MW (kDa)	alginic acid	EDC and Sulfo-NHS	PEG	antibody[b]	step 1	step 2
I	none	1	1	–	1	29/60	N/A
II	none	1	1	–	1	29/60	N/A
III	20	1	1	1	1	29/60	N/A
IV	10	1	1	1	1	29/60	N/A
V	10	2	1	1	1	29/0	29/60
VI	10	2	2	1	1	10/15	29/60
VII	10	2	2	1	1	29/60	29/60

[a] "1" denotes reagent added in step 1; "2" denotes reagent added in step 2. [b] Inert IgG was used for gel type I; antihuman CD34 was used in all other gel types.

mL) were added to 2 mL of MES buffer, mixed as before, and incubated for 60 min. For gel type III, 45 mg of alginic acid, 4.8 mg of EDC, 13.2 mg of sulfo-NHS, 45 mg of 20K MW PEG, and 100 μL of antihuman CD34 were added to 2 mL of MES buffer, mixed for 29 min, and allowed to incubate for 60 min. Gel type IV consisted of 45 mg of alginic acid, 4.8 mg of EDC, 13.2 mg of sulfo-NHS, 22.5 mg of 10K MW PEG, and 100 μL of antihuman CD34 added to 2 mL of MES buffer, mixed for 29 min, and allowed to incubate for 60 min. Gel type V was created by mixing 4.8 mg of EDC, 13.2 mg of sulfo-NHS, 22.5 mg of 10K MW PEG, and 100 μL of antihuman CD34 in 2 mL of MES buffer for 29 min and then adding 45 mg of alginic acid followed by 29 min of mixing and 60 min of incubation. Gels VI and VII were formed by mixing 22.5 mg of 10K MW PEG with 100 μL of antibody in 2 mL of MES buffer and mixing for 10 and 29 min, respectively, and incubating for an additional 15 and 60 min, respectively. Then, 4.8 mg of EDC, 13.2 mg of sulfo-NHS, and 45 mg of alginic acid were added to the mixture, mixed for 29 min, and allowed to incubate for 60 min. All formulations were mixed at room temperature (rt) and stored at 4 °C prior to use.

Following the incubation step, each functionalized alginic acid solution for each gel type was injected into a Slide-A-Lyzer dialysis cassette 10 000 molecular weight cutoff (Fisher) and dialyzed against MES buffer for 48 h to remove unreacted sulfo-NHS and EDC. Table 1 summarizes the synthetic steps and components for each gel type. Steps 1 and 2 indicate the sequential nature of the protocol followed for combining the respective reagents.

Infrared Spectroscopy. Functionalized alginic acid samples were spread on poly(tetrafluoroethylene) (PTFE) sample cards (Crystal Laboratories, Garfield, NJ) using a spatula and allowed to thicken for 4 h. The cards were then inserted into a Perkin-Elmer 1000 Fourier-transform infrared (FTIR) spectrometer (Waltham, MA). The absorbance at 638 cm^{-1}, corresponding to amide groups, was analyzed and compared for each gel type.

In Situ Hydrogel Formation within Microfluidic Devices. A 1 g/mL solution of $CaCl_2$ in deionized water was injected into each device (by hand, using a 1 mL syringe) and allowed to incubate overnight at rt. The $CaCl_2$ solution was then withdrawn by hand using a 1 mL syringe. The PEG- and antibody-functionalized alginate solution prepared for each gel type was then injected into the devices by hand and allowed to adsorb for 1 h. Next, the devices were rinsed with MES buffer at 10 μL/min for 10 min using a Harvard Apparatus PHD 2000 syringe pump (Holliston, MA), followed by a 100 mM $CaCl_2$ solution in MES buffer at 10 μL/min for 10 min to form a thin layer of hydrogel on the walls of the microchannels. Finally, the devices were rinsed with MES buffer at 10 μL/min for 10 min to remove unreacted $CaCl_2$. All experiments were conducted at rt.

BCA Protein Assay. A BCA protein assay solution was prepared according to the manufacturer's instructions. The solution was then injected into each device at 5 μL/min for 40 min at rt. The output was collected in a microplate and absorption at 562 nm was measured using a Bio-Tek Powerwave XS spectrometer (Winooski, VT).

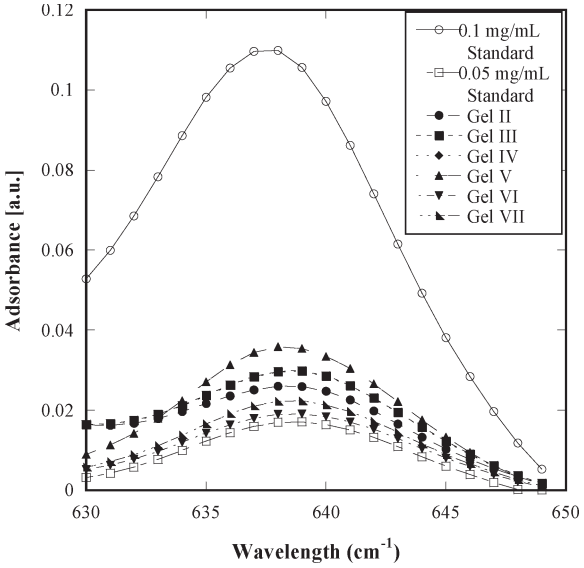

Figure 2. Infrared spectra of PEG- and antibody-functionalized hydrogels (gel types II–VII; not normalized to avoid total overlap) compared to standard solutions of anti-CD34 with concentrations of 0.1 and 0.05 mg/mL. The relative intensities of the hydrogel sample peaks are comparable, indicating similar levels of amide group content. Note that this measurement is a bulk measurement that does not distinguish between covalently bound antibody from antibody molecules that are physically trapped within the hydrogels.

Blood Draw. Whole human blood was drawn from healthy volunteers in heparin collection tubes under a protocol approved by the Northeastern University Institutional Review Board.

EPC Capture Protocol. Whole blood was injected into microfluidic capture devices at 5 μL/min for 60 min. Each device was then rinsed with MES buffer at 10 μL/min for 10 min. For release of captured cells, a 50 mM solution of EDTA in PBS was injected at 10 μL/min for 10 min and the output was collected in a 1.5 mL microcentrifuge tube. Devices were kept at rt for all cell release steps. Each individual experiment included 10 microfluidic devices, and 300 μL of blood was passed through each device, at the rate specified above. The cells released from each device were pooled into a single suspension to allow enumeration by a Beckman Coulter Quanta SC (Brea, CA) flow

dx.doi.org/10.1021/la105016a |*Langmuir* 2011, 27, 4257–4264

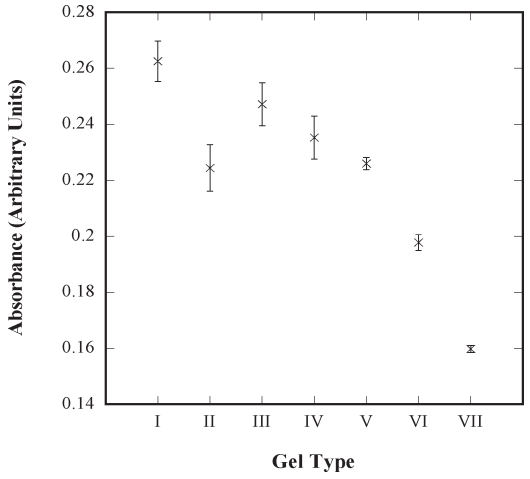

Figure 3. Qualitative measurement of accessible antibody within hydrogel-coated microfluidic devices. A bicinchoninic acid (BCA) assay kit was utilized to measure the relative amount of antibody accessible to a solution flowing through each device. A lower absorbance is associated with a greater amount of accessible antibody. Error bars denote standard errors based on eight independent measurements for each gel type.

cytometer. Hence, the data reported in Figure 4a,b represent yield and purity for EPCs recovered from a total blood volume of 3 mL.

Flow Cytometry. For EPC enumeration, cells released from each device were mixed with 10 μL each of antihuman CD133-PE, antihuman CD45-FITC, goat antihuman Flk-1, and antigoat IgG-PerCP. The mixture was stored in the dark at rt for 30 min followed by centrifugation at 130*g* for 10 min. The supernatant was decanted, and cells were suspended in 200 μL of PBS for enumeration using flow cytometry. While there is some debate as to the precise surface marker profile of EPCs, a general definition based on a number of literature sources[16−18] was applied in the present study, and released cells that were CD133+, CD45−, and Flk-1+ were counted as EPCs.[19−23]

RESULTS

Figure 2 shows infrared (IR) spectroscopy data for the functionalized alginic acid solutions emerging from the one- or two-step synthesis protocol. The spectra for gel types II−VII show equivalent levels of amide group content. In all of these gels, amide groups can result not only from binding between antibody and PEG molecules but also from antibody−alginic acid and PEG−alginic acid binding. The IR spectroscopy analysis therefore reflects that antibody and amide bond content, taken together, is very similar across all gel types, indicating successful incorporation of antibody and PEG; however, no functional distinctions between the different gel types can be predicted from these data.

Figure 3 shows relative total protein measurements made using a BCA assay kit. The BCA solution changes from green to blue as it comes in contact with proteins such as antibodies. Hence, by flowing this solution through hydrogel-coated microfluidic devices, the amount of accessible antibody on each gel type can be compared. The color change of the solutions exiting the devices is shown as a function of gel type in Figure 3 and is expressed in arbitrary units of absorbance at 562 nm rather than as a calibrated mass or concentration. Such a calibration cannot be performed, as the interaction between the BCA solution and protein is a flow-surface interaction, whereas standard calibrations would be carried out by mixing and incubating together the BCA solution and a solution of known protein concentration. The relative measurement nevertheless allows comparison of the accessible anti-CD34 capture antibody between each gel type. Figure 3 shows an increase in accessible antibody from gel types I−VII, while the total antibody and amide content of the mixture remains constant (Figure 2), indicating an increase in the efficiency of conjugation between the gelled surface and the antibody.

Figure 4 shows yield and purity data for the capture of EPCs from whole blood using the hydrogel-coated microfluidic devices. In Figure 4a, gel type I, which has an inert antibody conjugated to it, shows negligible EPC adhesion, as expected. Gel type II, which contains the anti-CD34 antibody, shows significantly higher EPC adhesion relative to gel type I ($p < 0.005$), albeit with a high degree of scatter. The purity of capture achieved with gel type II is, however, relatively low (∼23%; Figure 4b). The effect of adding the four-arm PEG to the hydrogel structure is shown clearly by comparing gel types II and IV, whose synthesis protocol is otherwise identical. The branched amine termini of the four-arm 10K MW PEG molecules provide an opportunity for a greater level of antibody conjugation, as reflected in the higher overall EPC adhesion (Figure 4a). The suppression of nonspecific binding results in an increase in purity (Figure 4b; gel type IV). Interestingly, the use of 20K MW PEG (gel type III) resulted in significantly lower EPC capture yield relative to 10K MW PEG (gel type IV; $p < 0.005$) under the same synthesis conditions, and purity levels were comparable.

In gel types V−VII, a two-step protocol for combining reagents was followed. In gel type V, the conjugation of the antibody molecules to the four-arm PEG is carried out first before introducing alginic acid. This formulation improved yield and purity of EPC capture relative to gel type IV. However, this protocol introduces the possibility of all four arms of the PEG molecules being occupied by antibodies, leaving no amine groups to bind to alginic acid. To address this risk, the two-step protocol was modified such that EDC and sulfo-NHS were added in the second step with alginic acid and the first step was restricted to the mixing together of PEG and antibody. When short times were provided for mixing and incubation for the first step (10 and 15 min, respectively, for gel type VI), the yield did not improve relative to gel type V; however, purity was marginally higher. Higher mixing and incubation times were examined next (29 and 60 min, respectively, for gel type VII) in an effort to achieve greater mixing and entanglement of the PEG molecules with the antibody molecules. This formulation provided significantly higher yields and purity relative to gel types VI and VII ($p < 0.005$ and $p < 0.01$, respectively). For all gel types, the viability of captured and released cells, as measured by Trypan Blue exclusion, was approximately 90%.

DISCUSSION

The ability to selectively capture and then release cells within microfluidic channels requires a balance of physical forces and chemical interactions[11] while simultaneously maintaining cell viability and function, particularly in the context of tissue engineering and regenerative medicine, where cell isolation is a common initial step.[24−26] Alginate hydrogels are particularly interesting for this application, because of the ability to easily create them by physical cross-linking of alginic acid in the presence of divalent cations and their well-known ability to

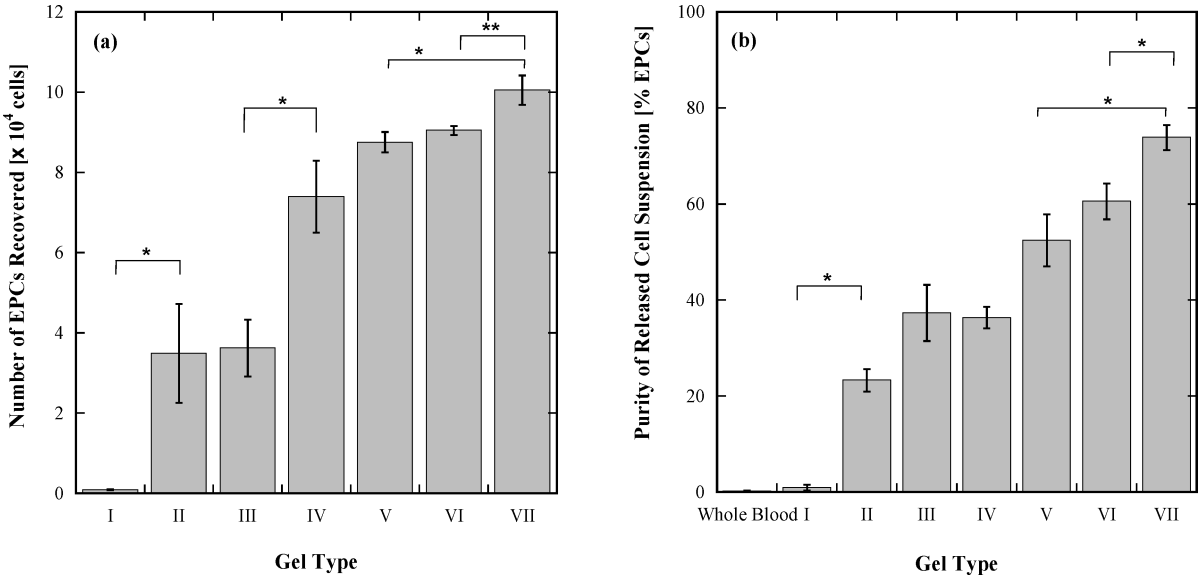

Figure 4. Yield (a) and purity (b) of EPCs captured from whole blood within microfluidic devices coated with PEG- and antibody-functionalized hydrogels. Whole blood (300 μL) collected in heparin tubes was directly injected into individual microfluidic devices and 10 devices were run in parallel. Cells released from each device were pooled into a single suspension to allow enumeration by flow cytometry. Data reported in parts a and b represent yield and purity for EPCs recovered from a total blood volume of 3 mL. Error bars denote standard deviations based on three independent measurements of EPC and total cell counts made with the same sample.

dissolve in the presence of chelators.[27−29] Furthermore, these hydrogels are biocompatible[30−32] and can be functionalized with cell-adhesive molecules.[12,33−36] Alginate hydrogels are, however, highly prone to nonspecific cell adhesion;[31] for example, in a recent study by our group that examined the capture of fibroblasts by alginate hydrogels, there was appreciable cell adhesion to the nonfunctionalized hydrogel.[12] When alginate hydrogels were functionalized with anti-CD34, a capture molecule for EPCs[37] utilized for EPC capture from whole blood, similar results were obtained in the form of high nontarget cell adhesion (results not shown). The present study was motivated by these observations and the hypothesis that the inclusion of PEG within the hydrogel structure would be a possible means to overcome this problem. Another shortcoming associated with functionalization of alginate hydrogels is the limited number of carboxylic acid groups available for carbodiimide-based conjugation. In the context of microfluidic capture devices, this limitation is exacerbated by the fact that flowing cells only "see" the adhesive capture molecules on the surface, whereas conjugation protocols are easiest to carry out in the bulk prior to hydrogel formation within the microchannels.[12]

PEG is well-known for its biological nonadhesiveness,[38−41] and the present study demonstrates how these properties can be harnessed while simultaneously increasing the capture molecule content of the hydrogel. These objectives are achieved by the use of four-arm PEG molecules with primary amine terminations at the end of each arm. In an ideal case, one arm of each four-arm PEG molecule would bind to a carboxylic acid group to the alginate hydrogel backbone, leaving up to three primary amine groups for antibody functionalization, provided the four-arm PEG is sufficiently large to prevent steric hindrance between adjacent antibody molecules. This arrangement would, in principle, triple the antibody content of the hydrogel and provide protection against nonspecific cell binding relative to non-PEG-ylated alginate hydrogels. However, such an idealized architecture is difficult to achieve synthetically if the same carbodiimide chemistry is to be utilized for both hydrogel−PEG and PEG−antibody binding. The present study examined how variations of a relatively simple synthetic protocol, made using probabilistic as well as chemical considerations, can overcome this constraint and provide effective capture and release of EPCs from whole blood. Protecting groups, such as fluorenylmethyloxycarbonyl chloride (fmoc),[42] can be effectively employed to achieve some level of control over protein or antibody conjugation to primary amine groups; however, here again it is difficult to ensure that only a certain number of amine groups are protected on each PEG molecule.

The need for simplicity in the hydrogel synthesis protocol arises from the intended application of these hydrogels in low-cost microfluidic cell separation systems for tissue engineering and clinical diagnostics. The present work, for example, provides the design basis for a microfluidic separator of EPCs from blood for subsequent use in vascular tissue engineering[43,44] or cell-based regenerative repair of vascular tissue in vivo.[43,45,46] Hence, there is significant motivation for keeping the number of synthesis steps and reagents to a minimum.

Figure 4 illustrates the evolution in synthetic protocols from gel types I−VII. The adhesive effect of the anti-CD34 antibody is evident by comparing gel types I and II (Figure 4a). Increased yield and purity are observed with the incorporation of 10K MW PEG (gel types II vs IV), while the level of scatter remains relatively large. The large error bars in both instances reflect the random nature of bond formation between the alginate hydrogel and the amine group-containing antibody and PEG molecules. As shown pictorially in Figure 5a, it is likely that the four-arm PEG molecules remain entangled in clusters, which would result in a patchlike accumulation of these clusters within the hydrogel, with antibody molecules being bonded within the clusters as well as directly to alginic acid. Such irregular distribution of antibody molecules would give rise to relatively large variations in cell adhesion between hydrogel samples that are otherwise identical

dx.doi.org/10.1021/la105016a |*Langmuir* 2011, 27, 4257–4264

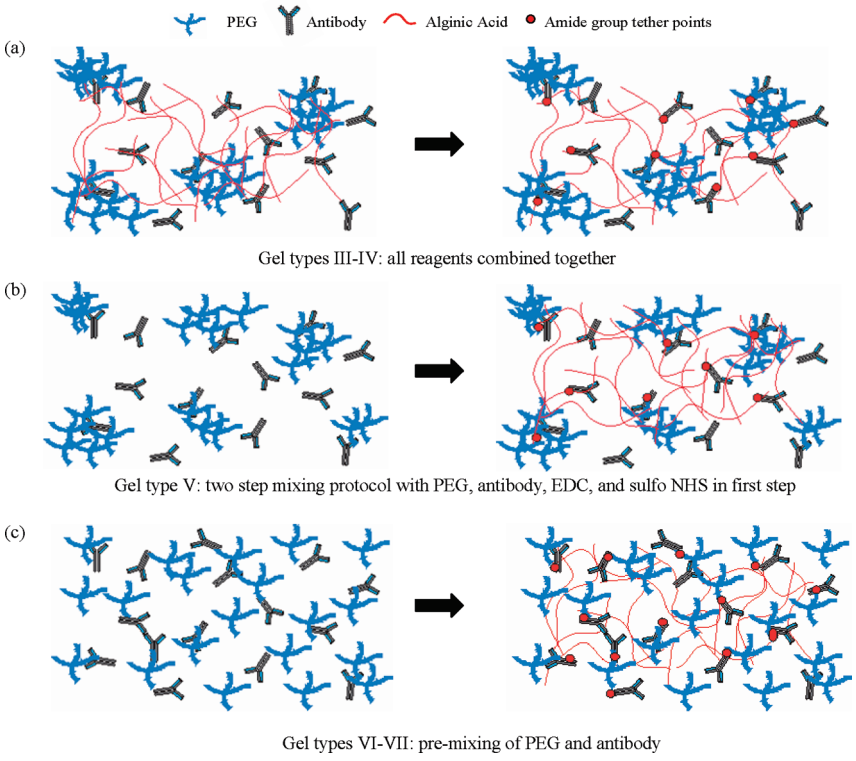

Figure 5. Illustration of structural differences in gel types. The left side of the figure is representative of mixing step 1 prior to the formation of amide bonds via EDC chemistry, and the right side represents the product resulting from mixing step 2 (see also Table 1). The progressive improvement in EPC capture yield and purity from gel types III−VII is attributed to the two-step mixing protocol, where PEG and antibody are premixed before the introduction of alginic acid and the coupling reagents EDC and sulfo-NHS. Premixing allows optimal dispersion of antibody molecules among the PEG chains.

with respect to reactants and method of combination. Indeed, the alginic acid solutions obtained after the two synthetic steps for gel types II and IV contained small particles of PEG visible to the naked eye (see light micrographs in Supporting Information), corroborating the hypothesis of inadequate mixing.

Each gel type is injected into a microfluidic device and subjected to identical flow and shear conditions. Slight variations in gel viscosity may impact the gel thickness within the device; however, due to the geometry of the post array, even a 3-fold difference in gel thickness will impact the overall surface area by less than 6% (see detailed calculation in the Supporting Information). The differences in capture efficiency between gel types is far greater than 6%, and it is therefore reasonable to argue that gel composition plays a much stronger role than gel thickness in the present context.

It is interesting to note that 20K MW PEG did not provide better capture and yield properties. Intuitively, one might expect the larger chains to provide a greater degree of steric freedom to antibody molecules bound to the amine termini and a greater resistance to nonspecific binding (i.e., greater purity). However, the results in Figure 4 indicate lower yield and comparable purity relative to hydrogels containing 10K MW PEG (gel types III vs IV). Both of these hydrogels have similar levels of antibody accessible to the BCA reagents (Figure 3), indicating chemical structure similarity. Hence, the more likely explanation for this difference is a physical structure difference wherein antibody molecules are farther apart from each other in the 20K PEG-containing hydrogel than in the 10K PEG-containing hydrogel. The antibody molecules are far enough apart that their probability of encountering a flowing EPC and their ability to capture it are both lower with 20K PEG. On this basis, 10K PEG was utilized in all subsequent formulations.

With gel type V, the first step in the synthesis was the combination of PEG and antibody with the coupling agents EDC and sulfo-NHS prior to the addition of alginic acid in the second step. Relative to gel type IV, gel type V provides slightly greater EPC capture, but with a lower degree of scatter, indicating better mixing of the antibody molecules with the PEG. The accessible antibody content of gel type V is similar to that of gel type IV (Figure 3), providing credence to the postulate of better PEG-antibody mixing being the distinguishing factor. Better mixing also allows for more effective interspersing of PEG and antibody molecules on the hydrogel surface, which is consistent with the higher EPC purity obtained with gel type V relative to gel type IV. Fewer PEG particles were observed in the PEG- and antibody-functionalized alginic acid solution, consistent with this postulate.

The two-step synthesis protocol for gel types VI and VII is built on the concept of better premixing by providing time for antibody and PEG molecules to mix "undisturbed" without the constraining presence of EDC and sulfo-NHS. Here, the longer mixing time provided alginic acid solutions that were visually clear, indicating good mixing, and the resulting coatings provided better EPC capture performance in terms of yield and purity relative to gel type V. The longer mixing and incubation times provided for gel type VII relative to gel type VI provided the best yield ($\sim 10^4$ EPCs recovered) and purity (74%).

Figure 4a does not show a comparison between EPC capture yields obtained with the hydrogels and the EPC content of whole

dx.doi.org/10.1021/la105016a |*Langmuir* 2011, 27, 4257–4264

blood. Flow cytometry measurements in our laboratory indicate a typical EPC count of 33×10^4 EPCs per 3 mL of whole blood for the samples used in this study. Hence, the best performing gel type in this work only captures about one-third of the total available EPC content. However, it important to note that this level of capture was achieved with only a single pass of the blood sample through the hydrogel-coated microfluidic devices. Series operation of multiple capture devices or sample recycling would offer a facile means to increase total yield. Stagewise separation could be employed to increase the purity of captured EPCs beyond the 74% level achieved with gel type VII in a single pass. These considerations are outside the scope of the present work, where the focus was limited to the design and synthesis of the capture coating material.

CONCLUSIONS

Alginate hydrogels functionalized with four-arm PEG molecules and antibodies can be utilized for effective capture and release of EPCs from whole blood in microfluidic devices. Providing adequate opportunity for the four-arm, amine-terminated PEG to mix with the anti-CD34 antibody prior to covalent attachment of both species to alginic acid via carbodiimide chemistry is essential to maximize the yield and purity of EPC capture. The significance of this work lies in the ability to achieve such capture and release from a complex, heterogeneous cell suspension using a relatively simple synthesis protocol. This capture/release approach can potentially be extended to the isolation of other rare cells from complex solutions, such as stem or progenitor cells from digested tissue.

ASSOCIATED CONTENT

Supporting Information. Light micrographs of particles in some functionalized alginic acid solutions and sensitivity analysis calculation to examine the impact of hydrogel coating thickness on the available surface area for cell capture. This material is available free of charge via the Internet at http://pubs.acs.org.

AUTHOR INFORMATION

Corresponding Author
*E-mail: smurthy@coe.neu.edu.

ACKNOWLEDGMENT

The authors gratefully acknowledge support from the National Institutes of Health and the National Science Foundation under grants R01-EB009327 and CBET 0932195, respectively, to S.K.M. The authors also thank Prof. Rebecca Carrier for access to the ultraviolet spectrometer, Prof. Elizabeth Klings for assistance with blood draws, and Prof. Jennifer West for insightful discussions on promoting hydrogel adhesion to PDMS.

REFERENCES

(1) Cheng, X. H.; Gupta, A.; Chen, C. C.; Tompkins, R. G.; Rodriguez, W.; Toner, M. *Lab Chip* **2009**, *9* (10), 1357–1364.

(2) Cheng, X. H.; Irimia, D.; Dixon, M.; Sekine, K.; Demirci, U.; Zamir, L.; Tompkins, R. G.; Rodriguez, W.; Toner, M. *Lab Chip* **2007**, *7* (2), 170–178.

(3) Nagrath, S.; Sequist, L. V.; Maheswaran, S.; Bell, D. W.; Irimia, D.; Ulkus, L.; Smith, M. R.; Kwak, E. L.; Digumarthy, S.; Muzikansky, A.; Ryan, P.; Balis, U. J.; Tompkins, R. G.; Haber, D. A.; Toner, M. *Nature* **2007**, *450* (7173), 1235–U10.

(4) Kotz, K. T.; Xiao, W.; Miller-Graziano, C.; Qian, W. J.; Russom, A.; Warner, E. A.; Moldawer, L. L.; De, A.; Bankey, P. E.; Petritis, B. O.; Camp, D. G.; Rosenbach, A. E.; Goverman, J.; Fagan, S. P.; Brownstein, B. H.; Irimia, D.; Xu, W. H.; Wilhelmy, J.; Mindrinos, M. N.; Smith, R. D.; Davis, R. W.; Tompkins, R. G.; Toner, M. Inflammation Host Response, I. *Nat. Med.* **2010**, *16* (9), 1042–U142.

(5) Doyle, P. S.; Bibette, J.; Bancaud, A.; Viovy, J. L. *Science* **2002**, *295* (5563), 2237–2237.

(6) Gleghorn, J. P.; Pratt, E. D.; Denning, D.; Liu, H.; Bander, N. H.; Tagawa, S. T.; Nanus, D. M.; Giannakakou, P. A.; Kirby, B. J. *Lab Chip* **2010**, *10* (1), 27–29.

(7) Wankhede, S. P.; Du, Z.; Berg, J. M.; Vaughn, M. W.; Dallas, T.; Cheng, K. H.; Gollahon, L. *Biotechnol. Prog.* **2006**, *22* (5), 1426–1433.

(8) Zhang, X.; Jones, P.; Haswell, S. J. *Chem. Eng. J.* **2008**, *135* (Supplement 1), S82–S88.

(9) Fujioka, N.; Morimoto, Y.; Takeuchi, K.; Yoshioka, M.; Kikuchi, M. *Appl. Spectrosc.* **2003**, *57* (2), 241–243.

(10) Jung, K.; Hampel, G.; Scholz, M.; Henke, W. *Cell. Physiol. Biochem.* **1995**, *5* (5), 353–360.

(11) Murthy, S. K.; Radisic, M., Cell Adhesion and Detachment. In *Encyclopedia of Microfluidics and Nanofluidics*; Li, D., Ed.; Springer: New York, 2008.

(12) Plouffe, B. D.; Brown, M. A.; Iyer, R. K.; Radisic, M.; Murthy, S. K. *Lab Chip* **2009**, *9* (11), 1507–1510.

(13) Kaushal, S.; Amiel, G. E.; Guleserian, K. J.; Shapira, O. M.; Perry, T.; Sutherland, F. W.; Rabkin, E.; Moran, A. M.; Schoen, F. J.; Atala, A.; Soker, S.; Bischoff, J.; Mayer, J. E. *Nat. Med.* **2001**, *7* (9), 1035–1040.

(14) Gatest, G. J.; Phillips, J. A. *Biotechnol. Tech.* **1992**, *6* (6), 517–522.

(15) Sawhney, A. S.; Pathak, C. P.; Hubbell, J. A. *Biomaterials* **1993**, *14* (13), 1008–1016.

(16) Chen, C.; Zeng, L.; Ding, S.; Xu, K. *Transplant. Proc.* **2010**, *42* (9), 3745–3749.

(17) Eggermann, J.; Kliche, S.; Jarmy, G.; Hoffmann, K.; Mayr-Beyrle, U.; Debatin, K. M.; Waltenberger, J.; Beltinger, C. *Cardiovasc. Res.* **2003**, *58* (2), 478–486.

(18) George, J.; Shmilovich, H.; Deutsch, V.; Miller, H.; Keren, G.; Roth, A. *Tissue Eng.* **2006**, *12* (2), 331–335.

(19) Hristov, M.; Erl, W.; Weber, P. C. *Arterioscler. Thromb. Vasc. Biol.* **2003**, *23* (7), 1185–1189.

(20) Asahara, T.; Murohara, T.; Sullivan, A.; Silver, M.; vanderZee, R.; Li, T.; Witzenbichler, B.; Schatteman, G.; Isner, J. M. *Science* **1997**, *275* (5302), 964–967.

(21) Urbich, C.; Dimmeler, S. *Circ. Res.* **2004**, *95* (4), 343–353.

(22) Hristov, M.; Erl, W.; Weber, P. C. *Trends Cardiovasc. Med.* **2003**, *13* (5), 201–206.

(23) Leor, J.; Marber, M. *J. Am. Coll Cardiol.* **2006**, *48* (8), 1588–1590.

(24) Sorkin, M.; Wong, V. W.; Glotzbach, J. P.; Major, M.; Levi, B.; Longaker, M. T.; Gurtner, G. C. *J. Am. Coll. Surg.* **2010**, *211* (3), S65–S65.

(25) Peterbauer-Scherb, A.; van Griensven, M.; Meinl, A.; Gabriel, C.; Redl, H.; Wolbank, S. *J. Tissue Eng. Regen. Med.* **2010**, *4* (6), 485–490.

(26) Bosio, A.; Huppert, V.; Donath, S.; Hennemann, P.; Malchow, M.; Heinlein, U. A. O. *Engineering of Stem Cells*; Springer-Verlag: Berlin, 2009; Vol. 114, pp 23−72.

(27) Couperwh., I; McCallum, M. F. *Arch. Microbiol.* **1974**, *97* (1), 73–80.

(28) Kong, H. J.; Mooney, D. J. *Mechanical Properties of Bioinspired and Biological Materials*; Viney, C., Katti, K., Ulm, F. J., Hellmich, C., Eds.; 2005; Vol. 844, pp 313−318.

(29) Rowley, J. A.; Madlambayan, G.; Mooney, D. J. *Biomaterials* **1999**, *20* (1), 45–53.

(30) Jeon, O.; Powell, C.; Ahmed, S. M.; Alsberg, E. *Tissue Eng. Part A* **2010**, *16* (9), 2915–2925.

(31) Suarez-Gonzalez, D.; Barnhart, K.; Saito, E.; Vanderby, R.; Hollister, S. J.; Murphy, W. L. *J. Biomed. Mater. Res. Part A* **2010**, *95A* (1), 222–234.
(32) Yu, J. S.; Du, K. T.; Fang, Q. Z.; Gu, Y. P.; Mihardja, S. S.; Sievers, R. E.; Wu, J. C.; Lee, R. J. *Biomaterials* **2010**, *31* (27), 7012–7020.
(33) Alsberg, E.; Anderson, K. W.; Albeiruti, A.; Rowley, J. A.; Mooney, D. J. *Proc. Natl. Acad. Sci. U. S. A.* **2002**, *99* (19), 12025–12030.
(34) Cheetham, P. S. J.; Blunt, K. W.; Bucke, C. *Biotechnol. Bioeng.* **1979**, *21* (12), 2155–2168.
(35) Drury, J. L.; Boontheekul, T.; Mooney, D. J. *J Biomech Eng. Trans. ASME* **2005**, *127* (5), 891–891.
(36) Hermanson *Bioconjugate Techniques*; Academic Press: New York, 1996.
(37) Plouffe, B. D.; Kniazeva, T.; Mayer, J. E.; Murthy, S. K.; Sales, V. L. *FASEB J.* **2009**, *23* (10), 3309–3314.
(38) Chen, H.; Yuan, L.; Song, W.; Wu, Z. K.; Li, D. *Prog. Polym. Sci.* **2008**, *33* (11), 1059–1087.
(39) Heuberger, M.; Drobek, T.; Voros, J. *Langmuir* **2004**, *20* (22), 9445–9448.
(40) Unsworth, L. D.; Tun, Z.; Sheardown, H.; Brash, J. L. *J. Colloid Interface Sci.* **2006**, *296* (2), 520–526.
(41) Norde, W.; Gage, D. *Langmuir* **2004**, *20* (10), 4162–4167.
(42) Frutos, A. G.; Brockman, J. M.; Corn, R. M. *Langmuir* **2000**, *16* (5), 2192–2197.
(43) Rafii, S.; Lyden, D. *Nat. Med.* **2003**, *9* (6), 702–712.
(44) Wu, X.; Rabkin-Aikawa, E.; Guleserian, K. J.; Perry, T. E.; Masuda, Y.; Sutherland, F. W. H.; Schoen, F. J.; Mayer, J. E.; Bischoff, J. *Am. J. Physiol. Heart Circ. Physiol.* **2004**, *287* (2), H480–H487.
(45) Li, T. S.; Hamano, K.; Nishida, M.; Hayashi, M.; Ito, H.; Mikamo, A.; Matsuzaki, M. *Am. J. Physiol. Heart Circ. Physiol.* **2003**, *285* (3), H931–H937.
(46) Yang, C.; Zhang, Z. H.; Li, Z. J.; Yang, R. C.; Qian, G. Q.; Han, Z. C. *Throm. Haemostasis* **2004**, *91* (6), 1202–1212.